Journal of the Korean Electrochemical Society
Vol. 12, No. 1, 2009, 61-67

Comparison between CFD Analysis and Experiments According to Various PEMFC Flow-field Designs

Kang In Lee, Se Won Lee, Min Soo Park[†], Yong-Hun Cho[††], Yoon-Hwan Cho[††], Chong Nam Chu*, and Yung-Eun Sung[††,*]

School of Mechanical & Aerospace Engineering, Seoul National University, Shilimdong, Gwanakgu, Seoul 151-744, Korea

[†]*BK21 School for Creative Engineering Design of Next Generation Mechanical and Aerospace Systems, Seoul National University, San 56-1 Shinlim-dong, Gwanak-gu, Seoul, 151-744, Korea*

[††]*School of Chemical & Biological Engineering & Research Center for Energy Conversion and Storage, Seoul National University, Seoul 151-744, Korea*

(Received January 8, 2009 : Accepted February 18, 2009)

Abstract : Flow-field design has much influence over the performance of proton exchange membrane fuel cell (PEMFC) because it affects the pressure magnitude and distribution of the reactant gases. To obtain the pressure magnitude and distribution of reactant gases in five kinds of flow-field designs, computational fluid dynamics (CFD) analysis was performed. After the CFD analysis, a single cell test was carried out to obtain the performance values. As expected, the pressure differences due to different flow-field configurations were related to the PEMFC performance because the actual performance results showed the same tendency as the results of the CFD analysis. A large pressure drop resulted in high PEMFC performance. The single serpentine configuration gave the highest performance because of the high pressure difference magnitudes of the inlet/outlet. On the other hand, the parallel flow-field configuration gave the lowest performance because the pressure difference between inlet and outlet was the lowest.

Keywords : Polymer electrolyte membrane fuel cell, Computational fluid dynamics, Flow-field.

1. Introduction

PEMFC is a subject of much research. This is because the PEMFC has the advantages of high power density and low operation temperature. It can be applied in many different areas ranging from small electrical devices to automobiles.[1-4] PEMFC consists of several key parts: membrane electrode assembly (MEA), gasket, flow-field plate, and endplate. Among these parts, the role of the flow-field plate is important. Flow-field plates act as a current collector and supply reactants gases like hydrogen or air to MEA. It also removes products like water droplets from the cell.

Various flow-field designs are available, such as the single serpentine, multiple serpentine, parallel and interdigitated designs.[5] Many researchers have studied the effects of flow field design. Hsieh *et al.*[6] studied the effects of different operating parameters on the PEMFC performances of three different flow-field configurations (interdigitated, mesh, and serpentine). Shimpalee *et al.*[7] used the serpentine flow-field design with various numbers of gas paths to vary the gas path lengths. They also studied the effects of the rib and channel dimensions of a flow-field on PEMFC performance.[3] Tuver *et al.*[8] investigated the performance of the fractal flow field design and compared it with the performances of the serpentine and parallel designs.

As reported in previous publication,[3,6-8] a flow field design has much influence on PEMFC performance because it affects the pressure drop, the pressure distribution, and the velocity of the reactant gases. It also affects product removal. Among these affected factors, pressure is a major influential factor of PEMFC performance because the pressure drops and distri-

*E-mail: cnchu@snu.ac.kr; ysung@snu.ac.kr

butions of the gases affect the voltage of the PEMFC and the removal of products like excess water droplets etc.[9-11] For these reasons, the relationship between pressure and PEMFC performance has been studied extensively. However, there have been very few researches about the performance of the PEMFC for various flow field designs through the pressure drop and pressure distribution analysis.

In this study, the differences of pressure drop and pressure distribution according to the flow field design is studied with CFD analysis and the CFD analysis result is compared with the single cell test result. Five kinds of flow-field designs on the cathode side such as single serpentine, zigzag, multiple serpentine, parallel serpentine, and parallel designs, were used for this study.

The CFD analysis was used to simulate the gas flow within the flow channel and consequently, the magnitude and distribution of the pressure were obtained without additional measurement equipments. With the CFD analysis simulated results could be obtained simply and quickly for comparison with the experimental results.[12] Although the CFD analysis can show the pressure analysis results with these advantages, it is not enough to obtain the accurate PEMFC performance data. Much of the simulation was done to determine the PEMFC performance, however the limitations such as setting many suppositions, boundary condition errors, and computational analysis limitation on electrochemical reaction may result in inaccurate values that differ from the experimental PEMFC performance values. So in order to obtain the most accurate performance results, CFD analysis was done about pressure analysis and the single cell test was carried out to measure the performance of PEMFC in this study.

2. Experiment

2.1. Various flow field designs of the cathode

Five kinds of flow-field designs on the cathode side, which were simulated with CFD analysis, were the single serpentine, zigzag, multiple serpentine, parallel serpentine, parallel designs. All flow-fields were designed to have the same size channel dimensions. The channel dimensions were 1 mm (width) × 1 mm (depth). In the zigzag flow-field, the connecting channel which connects three channels was 2 mm wide. Parallel serpentine and parallel flow-fields had stem channels that split into 1 mm (width) × 1 mm (depth) channels. Stem channel dimensions were 3 mm (width) × 1 mm (depth). The magnitude and distribution of the air pressure on the cathode for the five different flow-fields with a stoichiometric factor of 4 were analyzed by CFD.

2.2. CFD analysis and assumptions

A commercial flow solver, FLUENT 6.3, was used to run the CFD analysis and the modeling of the five different kinds of flow-fields and mesh creating were carried out with GAMBIT 2.3.16. The mesh interval size was 0.5 and the meshing elements were the Tet/Hybrid type. For simplification the CFD analysis was performed under the following assumptions.

1. All air gas flow in the channel is laminar and steady.
2. Channel walls consist of four faces of gold plated aluminum.
3. Use of oxygen and water creation on the cathode were ignored.
4. The temperature in the channel was maintained at the operating temperature of 343 K. Temperature distribution was not considered.
5. The outlet pressure to ambient air was set to 0 Pascal (gauge pressure).
6. Channel walls were under non-slip condition.
7. A constant mass flow rate was imposed as an inlet boundary condition.[13]

For the boundary conditions, the inlet velocity of the reactant gas was calculated by equation 1.

$$\dot{m} = \rho V A \quad (1)$$

This equation shows the quantity of inlet mass per a second where ($\dot{m}$) is the mass flowrate, (ρ) is the fluid density, (V) is the component of fluid velocity perpendicular to area A, and (A) is the inlet area. The mass flowrate is prescribed from the stoichiometric number.

2.3. Single cell performance measurement

Single cell tests were done with a stoichiometric factor of 4, as was done in the CFD analysis. The schematic of the PEMFC model for the single cell test is illustrated in Fig. 1. Commercial MEA with an active area of 5 cm (height) × 5 cm (width) was used. The catalyst loading on the anode and cathode was 0.4 mg/cm^2 with Pt/C 40 wt.%. Teflon gaskets were placed on both sides of MEA to prevent gas leakage. Aluminum was used for the base material of the flow-field plates to collect the generated current from the MEA. MEA can be contaminated with metallic material if the plate corrodes and the contact resistance

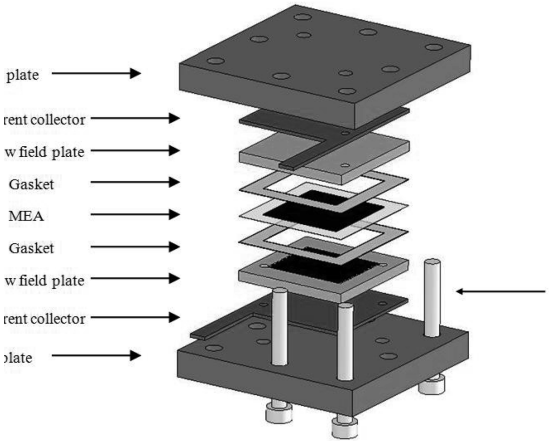

Fig. 1. The schematic of the PEMFC model for the single cell test.

increases due to the oxide layer on the surface of the flow-field plate.[14] To prevent these problems, the aluminum flow-field plates were plated with gold. Gold plating can enhance both cell performance and the corrosion resistance of the aluminum plate. The electrical performance of the gold plated aluminum plate is similar to graphite.[14] Flow field plates and gaskets and the MEA were sandwiched between two anodized aluminum endplates held together by eight bolts with a torque of 6 Nm on each bolt.

The single cell performance was measured by using hydrogen gas at 75°C with 100% relative humidity on the anode with a stoichiometric factor of 1.5.[15] On the cathode, air at 70°C with 100% relative humidity was supplied with stoichiometric factors of 4. The cell temperature during the single cell performance test was maintained at 70°C at ambient pressure throughout the experiments.[16] Counter flow direction was applied as default in this study. The current-voltage characteristics were measured using an electronic loader (WFCTS, WonATech Co., Ltd.).

3. Results and Discussion

3.1. CFD analysis results

For most fuel cells, mass transfer limitations due to oxygen transport are typically much more severe than the mass transfer limitation due to hydrogen transport. This is because air is typically used rather than oxygen and oxygen diffuses more slowly than hydrogen. For this reason, the flow field type is more crucial on the cathode side.[17] Therefore, the flow-field design on the anode was fixed as a multiple serpentine design so that the performance differences due to different flow-field designs on the cathode side could be observed. CFD analysis result of the five kinds of flow-field designs on the cathode side is shown Fig. 2.

The single serpentine flow-field had the highest pressure difference in inlet/outlet pressure among the five kinds of flow-field designs. The inlet pressure was 56402 Pascal and the outlet pressure was 0.05 Pascal. The air pressure continuously decreased along the channel from the inlet to the outlet. The average pressure of the entire area was 30302 Pascal. The analysis results of multiple serpentine and zigzag flow-fields gave similar magnitudes of the inlet/outlet pressure difference and pressure distribution. However, both the multiple serpentine and zigzag flow-fields yielded inlet/outlet pressure difference of less than 10% of that yielded by the single serpentine flow-field. The multiple serpentine configuration had a slightly lower pressure difference than the zigzag flow-field configuration: the Zigzag configuration gave a pressure difference of 5498 Pascal and the multiple serpentine configuration, 5001 Pascal. The average pressure of the entire area of the zigzag configuration was 2792 Pascal and that of the multiple serpentine configuration was 2527 Pascal. In some minute regions of the zigzag and multiple serpentine flow fields, minus gage pressure was seen. This phenomenon occurred at the very small region where three channels joined near the channel outlet. Thus this region did not have influence on air vent. Both flow-fields showed that the air pressure decreased along the channel from the inlet to the outlet.

The magnitude of the inlet/outlet pressure difference given by the parallel serpentine configuration was 11.5% of that of the zigzag configuration (1.1% of that of the single serpentine configuration). The magnitude of the inlet/outlet pressure difference of the parallel serpentine flow-field was 633 Pascal, and the average pressure of the entire area was 393 Pascal. The parallel flow-field gave the lowest pressure difference and the average pressure of the five kinds of flow-fields. The magnitude of the inlet/outlet pressure difference of the parallel serpentine flow-field was 370 Pascal and an average pressure of the entire area was 256 Pascal. It was 69.2% of the pressure difference given by the parallel serpentine flow-field. Both the parallel serpentine and parallel flow-fields showed that the inlet pressure was small compared to those of the other flow-fields.

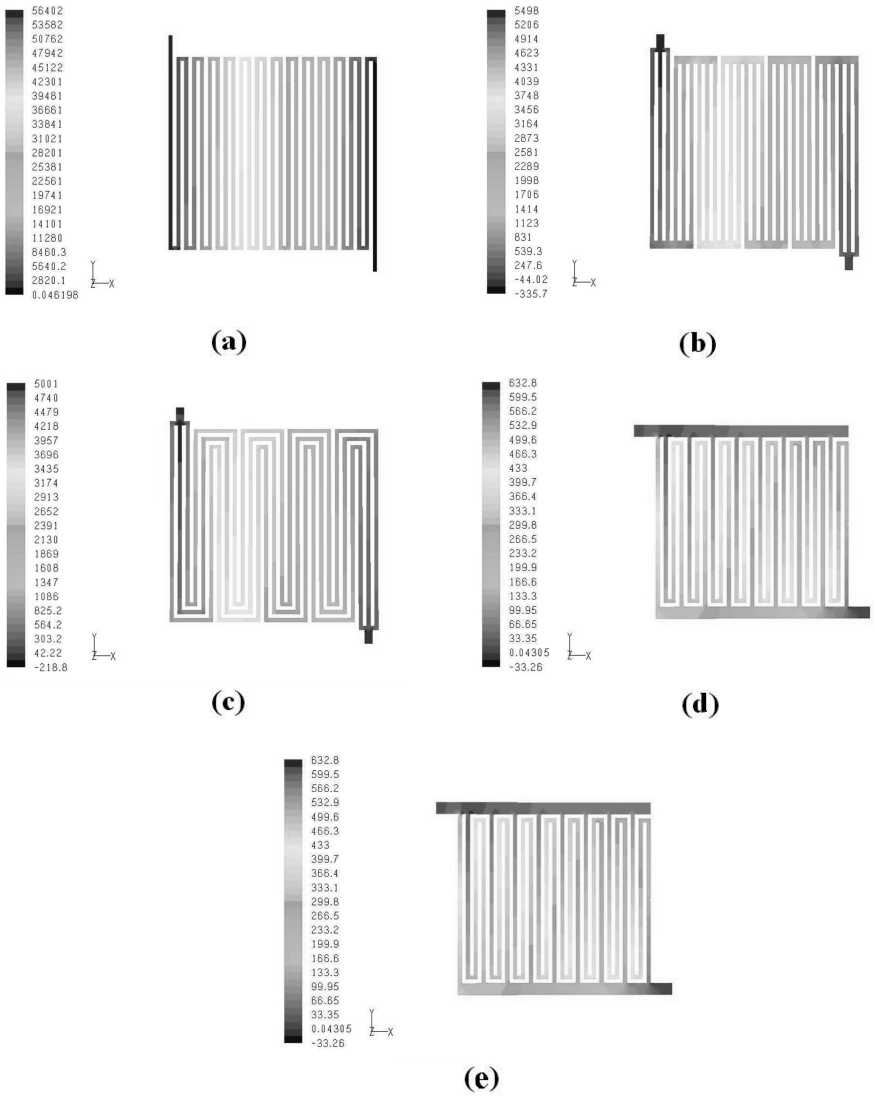

Fig. 2. CFD pressure analysis results with a stoichiometric factor of 4 according to cathode flow-field design: (a) single serpentine, (b) zigzag, (c) multiple serpentine, (d) parallel serpentine, (e) parallel.

The order of the magnitude of the inlet/outlet pressure difference of the five kinds of flow-fields were single serpentine >> zigzag ≥ multiple serpentine >> parallel serpentine > parallel. The same trend could be seen for the average pressure difference.

The pressure difference can change the cell voltage in the activation region and ohmic region. The Nernst equation can explain this effect.

$$E = E_0 + \frac{RT}{nF} ln\left(\frac{P_{H_2} P^{0.5}_{O_2}}{P_{H_2O}}\right) \quad (2)$$

This equation shows the Nernst equation of hydrogen/oxygen fuel cell reaction where (E) is the cell voltage, (E_0) is the voltage at standard temperature and pressure, (R) is the gas constant, (T) is the temperature, n is the number of electrons involved, (F) is the Faraday's constant, and (P) is the partial pressure of each gases.

a) An increase in the exchange current density due to increased concentration of reactant gases in the electrode. Exchange current density at pressure differs from reference/ambient pressure

$$i_0 = i_O^{ref}\left(\frac{P}{P_O}\right)^{\gamma} \quad (3)$$

where (i_0) represents the exchange current density, (i_O^{ref}) is the reference exchange current density, and (γ) is the pressure coefficient.

b) So the cell potential gain at an elevated pressure is

$$\nabla V = \frac{RT}{nF} ln\left[\left(\frac{P_{H_2}}{P_O}\right)\left(\frac{P_{O_2}}{P_O}\right)^{0.5}\right] + \frac{RT}{\alpha F} ln\left(\frac{P}{P_O}\right) \quad (4)$$

where (α) is the transfer coefficient.[18)]

For this reason, high pressure drop can cause an increase in cell voltage. So, the performance order of the five kinds of flow-field designs which is based on the inlet/outlet pressure difference would be the following: single serpentine >> zigzag ≥ multiple serpentine >> parallel serpentine > parallel, the same as shown in the CFD analysis result. The zigzag and multiple serpentine designs would be expected to show similar performance.

3.2. Comparison with PEM single cell data

Fig. 3 shows the I-V curve and power density curve of the single cell. The sequence of the performance was single serpentine >> zigzag ≥ multiple serpentine >> parallel serpentine > parallel. The single serpentine flow-field achieved the highest performance. The current density and the power density of the single serpentine flow-field at 0.6 V were 1.13 A/cm^2 and 0.68 W/cm^2. The performances of the zigzag and multiple serpentine flow-fields were similar; both being lower than that of the single serpentine flow-field. At 0.6 V the current density of zigzag and multiple serpentine flow fields were 0.797 A/cm^2 and 0.784 A/cm^2, and the power density were 0.478 W/cm^2 and 0.472 W/cm^2. The parallel serpentine flow-field had lower performance than the zigzag or multiple serpentine flow-fields. At 0.6 V the current density was 0.689 A/cm^2 and the power density was 0.414 W/cm^2. The parallel configuration gave the lowest performance. The current density of the parallel configuration at 0.6 V was 0.522 A/cm^2 and the power density was 0.314 W/cm^2.

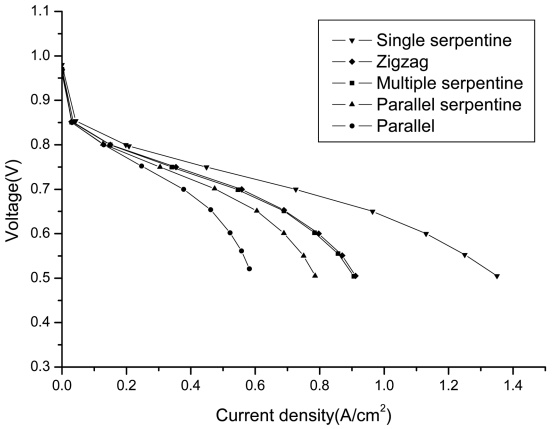

Fig. 3. Polarization curves with a stoichiometric factor of 4 according to cathode flow-field design: (a) single serpentine, (b) zigzag, (c) multiple serpentine, (d) parallel serpentine, (e) parallel.

This result shows that the performance order of the five kinds of flow-field designs was the same as seen in the CFD analysis results. The results indicate that the high pressure difference from inlet to outlet extended to the mass transfer limit region. Due to the extension of the mass transfer limit region, PEMFC obtained higher power density. It was remarkable that the single serpentine flow-field showed superior power density over all other flow-fields. This meant that the high pressure difference not only increased the cell voltage in the activation region and ohmic regions, but also extended the mass transfer limit region. This phenomenon can be explained as follows.

Increased pressure difference allowed more reactant gases to reach to the triple phase zone of MEA where the chemical reaction occurred. In the case of high current density, more oxygen was needed. So the accessibility of oxygen was sensitive at the condition of high current density. The mass transfer limit region of the single serpentine configuration was extremely extended, much more than those of the other configurations due to the high pressure difference. Unlike the flow-field of the single serpentine design, that of the parallel design reached the mass transfer region faster because of low oxygen accessibility. The zigzag and multiple serpentine designs had similar pressure difference and distribution. Therefore, both of these flow-fields reached the mass transfer limit region at a similar current density.

Gas transport mode was also affected by pressure difference. In the case of a low pressure difference produced by the parallel flow-field, the gas transport mode was the diffusion through the gas diffusion layer (GDL) only upon the arrival of the reactant gases at the electrolyte through the GDL. However in the case of a high pressure difference between channels, as in

the single serpentine design, convection, in addition to the diffusion through GDL, occurred between channels.[17] The gas transport mode by convection raised the accessibility of the reactant gases to the electrolytes; therefore, the mass transfer limit region was extended.

If water is not removed easily, the water within the channels interrupts the diffusion of the reactant gases to the active area. This interruption makes the PEMFC reach the mass transfer limit region quickly. In the case of the parallel flow-field, the product water can inhibit the transport of the reactant to the active area, decreasing performance.[8] On the contrary, the excess liquid water can be easily removed in the single serpentine flow-field by the high pressure drop. For this reason, the single serpentine flow-field had relatively high performance.

It was verified that flow field type greatly affected the performance of the PEMFC. If the pressure drop is not a major factor, using the single serpentine flow field design will yield the highest cell performance. The zigzag and multiple serpentine flow-fields had similar pressure drops in the CFD analysis result, as well as similar cell performances. The multiple serpentine and zigzag flow-fields are suitable when both the pressure drop and cell performance are important concerns. In the parallel serpentine flow-field, the pressure drop was low; however, the cell performance was also low. The parallel flow-field had lowest pressure drop and cell performance. If the pressure drop is a major factor, the parallel serpentine or parallel flow-field is recommended.

4. Conclusions

In this paper, the inlet/outlet pressure difference and pressure distribution among different flow-field designs were studied with CFD analysis and then by the single cell test to determine how the pressure difference affects the cell performance. the performance order of the five kinds of flow-field designs which is based on the inlet/outlet pressure difference was single serpentine >> zigzag ≥ multiple serpentine >> parallel serpentine > parallel. The single cell test showed that the actual performance results had the same tendency as the results of the CFD analysis. A large pressure drop resulted in high cell performance. The performance changed according to the flow-field because of the following reasons.

1. When the pressure increased, the cell voltage increased accordingly by the Nernst equation.

2. Increased pressure difference allowed more reactant gases to reach the triple phase zone of MEA where the chemical reaction occurs.

3. The high pressure difference between channels allowed gas to transport not only by diffusion but also by convection.

4. When the pressure drop was high, the excess water products were removed easily.

Acknowledgments

This work was financially supported by Korea Research Foundation (Grant # KRF-2004-005-D00064), KOSEF through the Research Center for energy Conversion and Storage, and National RD&D Organization for Hydrogen & Fuel Cell & Ministry of Commerce, Industry and Energy.

Nomenclature

A	Area of inlet channel (m^2)
E	Operating voltage (V)
E_0	Voltage at standard temperature and pressure (25 °C & 101.25 kPa)
F	Faraday's constant (96485 C/mol)
i_0	Exchange current density (A/m^2)
i_O^{ref}	Reference exchange current density (3×10^{-6} A/cm^2)
$\dot{m}$	Inlet mass per second (Kg/s)
P	Reactant partial pressure of each gases (kPa)
R	The gas constant (8.314 J/mol K)
T	Temperature (K)
V	Component of fluid velocity perpendicular to area A (m/s)

Greek symbols

α	Transfer coefficient
γ	Pressure coefficient
ρ	Gas density (Kg/m^3)

References

1. C. K. Dyer, 'Fuel cells for portable applications', J. Power Sources, **106**, 31 (2002).
2. A. Heinzel, C. Hebling, M. Müller, M. Zedda, and C. Müller, 'Fuel cell for low power applications', J. Power Sources, **105**, 250(2002).
3. S. Shimpalee and J. W. Van Zee, 'Numerical studies on rib & channel dimension of flow-field on PEMFC performance', Int. J. Hydrogen Energy, **32**, 842 (2007).
4. C. H. Cheng, K. Fei, and C. W. Hong, 'Computer simulation of hydrogen proton exchange membrane and

direct methanol fuel cells', Computers & Chemical Engineering, **31**, 247 (2007).
5. L. Wang and H. Liu, 'Performance studies of PEM fuel cells with interdigitated flow fields', J. Power Sources, **134**, 185 (2004).
6. S. S. Hsieh, S. H. Yang, J. K. Kuo, C. F. Huang, and H. H. Tsai, 'Study of operational parameters on the performance of micro PEMFCs with different flow fields', Energy conversion & Management, **47**, 1868 (2006).
7. S. Shimpalee, S. Greenway, and J. W. Van zee, 'The impact of channel path length on PEMFC flow-field design', J. power source, **160**, 398 (2006).
8. K. Tuber, A. Oedegaard, M Hermann, and C. Hebling, 'Investigation of fractal flow-fields in proton exchange membrane and direct methanol fuel cells', J. power source, **131**, 175 (2004).
9. X. Zhou, W. Ouyang, C. Liu, T. Lu, W. Xing, and L. An, 'A new flow field and its-two dimension model for polymer electrode membrane fuel cells (PEMFCs)', J. Power Sources, **158**, 1209 (2006).
10. X. Li and I. Sabir, 'Review of bipolar plates in PEM fuel cells: Flow-field designs', Int. J. Hydrogen Energy **30**, 359 (2005).
11. A. S. Aricò, P. Cretì, V. Baglio, E. Modica, and V. Antonucci, 'Influence of flow field design on the performance of a direct methanol fuel cell', J. Power Sources, **91**, 202 (2000).
12. V. A. Danilov, J. Lim, I. Moon, and H. Chang, 'Three-dimensional, two-phase, CFD model for the design of a Adirect methanol fuel cell', J. Power Sources, 162, **992** (2006).
13. G. Squadrito, O. Barbera, G. Giacoppo, F. Urbani, and E. Passalacqua, 'Computer aided fuel cell design and scale-up, comparison between medel and experimental results', J. Applied Electrochemistry, **37**, 87 (2007).
14. G. O. Mepsted and J. M. Moore, 'Performance and durability of bipolar plate materials', W. Vielstich, A. Lamm and H. A. Gasteiger (Eds.), "Handbook of Fuel Cells: Fundamentals Technology and Applications", Vol. 3, 286, John Wiley & Sons, New York (2003).
15. W. M. Yan, C. Y. Chen, C. C. Mei, C. Y. Soong, and F. Chen, 'Effects of operating conditions on cell performance of PEM fuel cells with conventional or interdigitated flow field, J. Power Sources', **162**, 1157 (2006).
16. Y. -H. Cho, H. -S. Park, Y. -H. Cho, D. -S. Jung, H. -Y. Park, and Y. -E. Sung, 'Effect of platinum amount in carbon supported platinum catalyst on performance of polymer electrolyte membrane fuel cell' J. Power Sources **172**, 89 (2002).
17. R. O'Hayre, S. W. Cha, W. Colella, and F. B. Prinz, "Fuel Cell Fundamentals", 146-166, John Wiley & Sons, New York (2006).
18. F. Babir, "PEM Fuel Cells: Theory and Practice", 55, Elsevier Academic Press, Burlington (2005).